CHEMISTRY OF MATERIALS

Article

pubs.acs.org/cm

Engineering the Shape of Block Copolymer Particles by Surface-Modulated Graphene Quantum Dots

Hyunseung Yang,[†] Kang Hee Ku,[†] Jae Man Shin,[†] Junhyuk Lee,[†] Chan Ho Park,[†] Han-Hee Cho,[†] Se Gyu Jang,[‡] and Bumjoon J. Kim*[,†]

[†]Department of Chemical and Biomolecular Engineering, Korea Advanced Institute of Science and Technology (KAIST), Daejeon, 305-701, Republic of Korea

[‡]Soft Innovative Materials Research Center, Korea Institute of Science and Technology (KIST), Jeonbuk, 565-905, Republic of Korea

Supporting Information

ABSTRACT: Surface-engineered, 10 nm-sized graphene quantum dots (GQDs) are shown to be efficient surfactants for producing 3-pentadecyl phenol (PDP)-combined poly(styrene-*b*-4-vinylpyridine) (PS-*b*-P4VP(PDP)) particles that feature tunable shapes and internal morphologies. The surface properties of GQDs were modified by grafting different alkyl ligands, such as hexylamine and oleylamine, to generate the surfactant behavior of the GQDs. In stark contrast to the behavior of the unmodified GQDs, hexylamine-grafted GQDs and oleylamine-grafted GQD surfactants were selectively positioned on the PS and P4VP(PDP) domains, respectively, at the surface of the particles. This positioning effectively tuned the interfacial interaction between two different PS/P4VP(PDP) domains of the particles and the surrounding water during emulsification and induced a dramatic morphological transition to convex lens-shaped particles. Precise and systematic control of interfacial activity of GQD surfactants was also demonstrated by varying the density of the alkyl ligands on the GQDs. The excellent surface tunability of 10 nm-sized GQDs combined with their significant optical and electrical properties highlight their importance as surfactants for producing colloidal particles with novel functions.

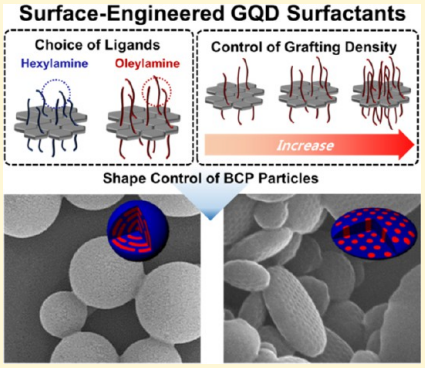

INTRODUCTION

Nanostructured polymeric particles have attracted significant attention as promising candidates for particle-based applications such as photonics, sensing devices, displays, and catalytic supports.[1−5] Block copolymers (BCPs) confined in small emulsion droplets could be especially useful in producing particles with unconventional nanostructures and surface properties.[6−23] The nanostructures of these particles can be controlled by changing the volume fraction of the blocks[10−12] and the particle size.[13,14] A critical parameter in determining the morphology within these confined droplets is the interfacial interaction between BCPs and the surrounding medium.[15,16,24] Compared to thin films or the bulk case, the interactions in confined droplets are magnified by the high surface area of particles relative to their volume, further expanding the richness of their morphological behavior.[24−26] For example, the morphological transition of BCP particles from onion-shaped to ellipsoid with axially stacked lamellae was observed by using mixed surfactants that neutralized the surface preference of each block in symmetric BCP to the surrounding medium.[15,16,27] Recently, Hawker's group[28] and our group[26] both demonstrated the effective use of Au nanoparticles (NPs) in modulating the surface properties of BCP particles, resulting in a dramatic transition in particle shape. The synthetic versatility in the precise tuning of the size of the NPs makes them more powerful in engineering BCP particles because the positioning of NPs at the surface of the BCP particles can be controlled in terms of their size and shape, highlighting their superior potential over traditional organic surfactants.[25,26,28] However, NPs typically have a spherical shape, which is not the optimal shape for maximizing their surfactant efficiency at the two-dimensional surface plane of polymer particles. The surfactant efficiency can be greatly amplified by using a NP with an alternative shape, such as a platelike shape.

Graphene quantum dots (GQDs), which are nanometer-sized graphene plates, have been the subject of intensive research due to their remarkable properties, such as biocompatibility and tunable luminescent behavior.[29,30] Recently, the use of GQDs as surfactants for stabilizing emulsion droplets has been reported.[31,32] And GQDs' size and shape offer great potential for their applications as particle surfactants. For example, the surfactant efficiency of GQD should be much higher than that of spherical-shaped NPs due to their platelike geometry.[33,34] In addition, unlike the micrometer-sized graphene oxide (GO) sheets, GQDs at ∼10 nm are smaller than the size of the BCP domains, enabling the selective tuning of the interfacial properties of the BCP particles by positioning the GQDs at the desired locations on the particle surface.

Received: October 31, 2015
Revised: January 9, 2016

DOI: 10.1021/acs.chemmater.5b04222
Chem. Mater. XXXX, XXX, XXX−XXX

Scheme 1. (a) Schematic Illustration for the Design of GQD Surfactants with Different Alkyl Ligands and Grafting Densities; (b) Fabrication of PS-*b*-P4VP(PDP)$_{0.5}$ Particles Stabilized by GQD Surfactants through Oil-in-Water Emulsion

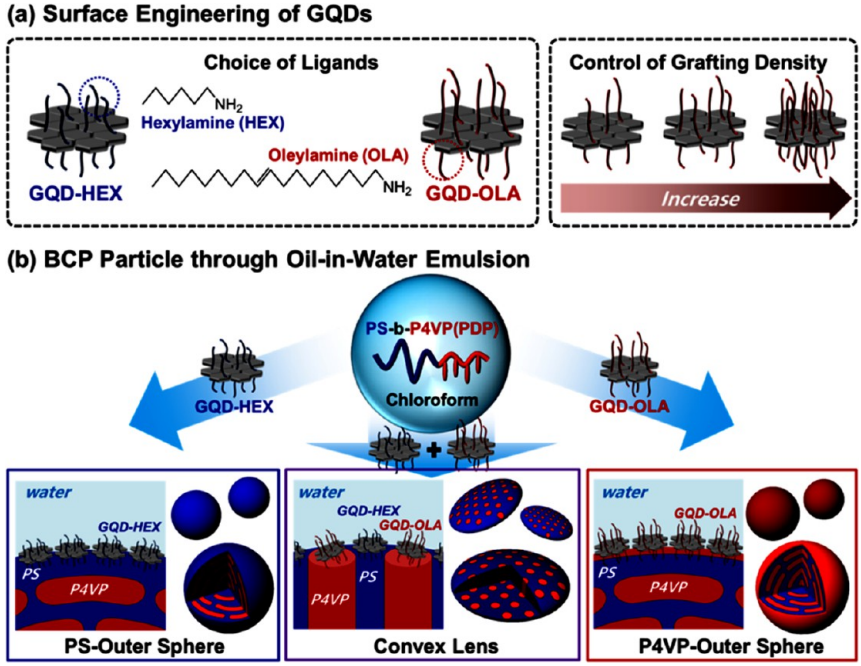

Furthermore, GQDs have hydrophobic π domains on the basal plane and abundant hydrophilic oxygen-containing groups, which can serve as reactive sites for surface modification.[31,35,36] Therefore, the surface properties of GQDs can be controlled easily through the facile grafting of small-molecular or polymeric ligands via cycloaddition, hydrophobic, and $\pi-\pi$ stacking interactions.[31,36−40]

Herein, we describe a facile and powerful strategy of using surface-engineered GQDs to produce the BCP particles with controlled external shapes and internal nanostructures. The addition of GQDs to colloidal particles containing cylinder-forming 3-pentadecyl phenol (PDP)-combined poly(styrene-*b*-4-vinylpyridine) (PS-*b*-P4VP(PDP)) results in a dramatic transition from a traditional spherical particles to convex lens-shaped particles (CL particles) with highly ordered and oriented nanoporous channels. The key to generating this morphological transition in the BCP particles is precise tuning of the surface properties of the GQDs using different types of alkyl ligands (i.e., hexylamine (HEX) and oleylamine (OLA)), which have preferential interactions with each block of PS-*b*-P4VP. While the GQDs modified with OLA (GQD-OLA) preferentially adsorb on the P4VP(PDP) domain at the surface of BCP particles, the GQDs modified with HEX (GQD-HEX) were selectively located at the PS domain, inducing neutral wetting of the PS and P4VP(PDP) domains at the particle surface and producing CL particles. Furthermore, the superior potential of GQD surfactants was demonstrated through tuning of surface properties by varying the OLA grafting densities on GQD. Overall, our surface-engineering method using GQDs can be an efficient strategy for modulating the interfacial properties at the surface of BCP particles and thus generating particles with the desired shapes and nanostructures.

EXPERIMENTAL SECTION

Materials. Vulcan CX-72 carbon black was purchased from Cabot Corporation. Concentrated nitric acid, oleylamine, and hexylamine were purchased from Aldrich. The PS-*b*-P4VP block copolymers (number average molecular weight (M_n) = 67 kg/mol, volume fraction of PS block (f_{PS}) = 0.75, polydispersity index (PDI) = 1.15) were purchased from Polymer Source, Inc. Deionized water (DI) was used in all experiments.

Synthesis of Alkylamine-Grafted GQDs. GQDs were synthesized via the chemical oxidation approach as described in previous work.[32,41] Briefly, carbon black was refluxed with concentrated nitric acid for 48 h. Then the solution was cooled to room temperature and centrifuged at 4000 rpm for 20 min. The supernatant was heated to yield a reddish-brown powder. GQDs were redispersed in tetrahydrofuran (THF) and ultrafiltered through a 0.22 μm microporous membrane; the fluorescent GQDs were obtained in the filtrate. To prepare alkylamine-grafted GQDs, hexylamine and as-prepared GQDs were dissolved in THF (10 mL) with nitrogen bubbling and the mixture was heated at 50 °C for 12 h. After the mixture was cooled to room temperature, THF was evaporated, and product was purified with diethyl ether to remove ungrafted hexylamine by repeated centrifugation at 4000 rpm for 10 min. The product was named GQD-HEX. A similar procedure was applied for the synthesis of GQD-OLA$_{0.2}$, GQD-OLA$_{0.4}$, and GQD-OLA$_{0.7}$ with different weight ratios of OLA to pristine GQDs.

Fabrication of BCP Particles. The PS-*b*-P4VP block copolymers were dissolved in chloroform to produce a 1 wt % polymer solution. Then the PDP molecules in chloroform were added to the PS-*b*-P4VP solution. The molar ratio of PDP to 4VP unit was fixed at 0.5. Various feed masses of GQD surfactants were added to the PS-*b*-P4VP-(PDP)$_{0.5}$ solution to produce feed volume fractions of GQDs ranging from 0 to 0.10. To estimate the volume of the alkylamine-grafted GQDs, the weight fractions of GQD and alkylamine ligands in the GQDs were measured by thermal gravimetric analysis (TGA) and their volume fractions were calculated by using the densities of hexylamine (0.77 g/cm^3), oleylamine (0.81 g/cm^3), and GQDs (1.80 g/cm^3). The volume fractions of PS-*b*-P4VP(PDP) polymers in the BCP particles were calculated from their feed masses by considering the densities of PS-*b*-P4VP (1.05 g/cm^3) and PDP (0.91 g/cm^3). After the addition of the GQDs with various alkylamine densities, the total solution (0.2 mL) was stirred for 24 h and emulsified in DI water (2.5 mL) containing 0.5 wt % of cetyltrimethylammonium bromide (CTAB) using a homogenizer for 1 min at 20000 rpm. Then chloroform was slowly evaporated at room temperature for 24 h. The sample was washed with DI water to remove the large excess of

DOI: 10.1021/acs.chemmater.5b04222
Chem. Mater. XXXX, XXX, XXX−XXX

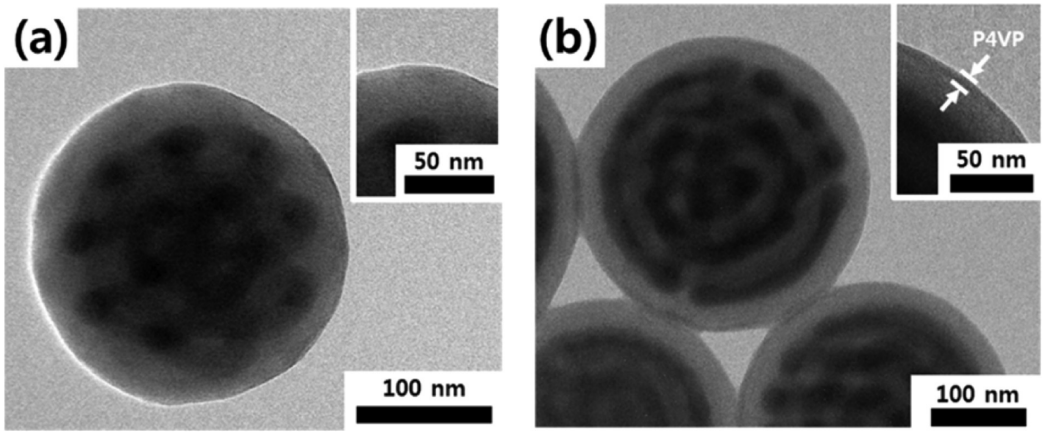

Figure 1. TEM images of PS-*b*-P4VP(PDP)$_{0.5}$ BCP particles stabilized by different GQD surfactants: (a) GQD-HEX$_{0.7}$; (b) GQD-OLA$_{0.7}$. GQD-HEX$_{0.7}$ produced BCP particles with PS as the outermost layer, whereas GQD-OLA$_{0.7}$ generated BCP particles with P4VP as the outermost layer. The P4VP domains appear darker after selective staining with iodine vapor.

remaining surfactants by repeated centrifugations performed at 13500 rpm for 10 min, and it was redispersed in DI water for further characterization.

Characterizations. Attenuated total reflectance-Fourier transform infrared spectroscopy (ATR-FTIR) spectra were taken using a Bruker ALPHA. X-ray photoelectron spectroscopy (XPS) spectra were taken using a Thermo VG Scientific ESCA 2000. Field emission scanning electron microscopy (SEM; Hitachi S-4800) and transmission electron microscopy (TEM; JEOL 2000FX) characterizations were performed to investigate the size of GQDs and the morphology of BCP particles. Samples for TEM measurements were prepared by dropping aqueous suspensions of GQDs or BCP particles onto Cu grids coated with a holey carbon film followed by solvent evaporation. The prepared samples were exposed to iodine vapor to selectively stain the P4VP domains of the PS-*b*-P4VP.

RESULTS AND DISCUSSION

Scheme 1 describes (a) the design of the GQD surfactants modified with different alkyl ligands and grafting densities (Σ) and (b) the control of the shape of the BCP particles using the GQD surfactants through the "emulsion-encapsulation and evaporation process". To prepare the GQD surfactants, we first synthesized 10 nm-sized GQDs using the method reported previously.[32,41] Then different alkyl ligands of HEX and OLA were attached to the surface of GQDs by the ring-opening reaction between epoxy moieties of GQDs and alkylamines, which was performed at the mild temperature of 50 °C (Scheme 1a).[31,36] Two different GQDs were synthesized to have similar Σ values of 0.7 chain/nm^2, which minimizes the effect of ligand density on the surface properties of the GQDs. For convenience, these GQDs are denoted as GQD-HEX$_{0.7}$ and GQD-OLA$_{0.7}$, respectively. The Σ values of alkyl ligands on the GQDs were estimated based on the relative weights of the GQDs and the alkylamine ligands on the GQDs (Table S1, Supporting Information). We compared the weight loss fraction of pristine GQD, GQD-HEX, and GQD-OLA after thermal cycle (25−650 °C) of thermogravimetric analysis (TGA) as shown in Figure S1, and we assumed that the difference in the weight loss was attributed to the grafting of the alkylamine ligands.[35,42] To further confirm the successful grafting of the alkylamine ligands on the GQDs, the average sizes of pristine GQD, GQD-HEX, and GQD-OLA were measured by TEM (Figure S2). The average size of the pristine GQDs was 10.4 ± 0.5 nm, while the sizes of the GQD-HEX$_{0.7}$ and GQD-OLA$_{0.7}$ were slightly increased to 11.2 ± 0.4 and 12.0 ± 0.6 nm, respectively. The increase in the sizes of the GQDs after the grafting reaction suggested the successful attachment of the alkylamine ligands to the surface of the GQDs.[31,35] The discrepancy in the average size between GQD-OLA$_{0.7}$ and GQD-OLA$_{0.7}$ might be attributed to the difference in the chain lengths of the HEX and OLA ligands. Covalent grafting of alkylamine ligands on the GQDs was also confirmed from the ATR-FTIR spectroscopy measurements. Compared to the pristine GQDs, the alkylamine-grafted GQDs were shown to have the C−H stretching of the alkylamine peak at both 2854 and 2927 cm^{-1} (Figure S3).

The emulsion-encapsulation and evaporation process was used to generate the BCP particles (Scheme 1b). The BCP colloidal particles were produced from a chloroform-in-water emulsion and subsequent evaporation of chloroform. PS-*b*-P4VP (M_n of PS block = 50 kg/mol; M_n of P4VP block = 17 kg/mol; PDI = 1.15) and PDP molecules were dissolved in chloroform. To promote favorable interaction between the GQDs and the BCP chains, PDP was added as a small-molecule linker to produce the complex of PS-*b*-P4VP(PDP)$_{0.5}$ with cylindrical morphology.[25,26,43] The mixture of PS-*b*-P4VP(PDP)$_{0.5}$ polymer solution in chloroform and GQD surfactants was emulsified in pure deionized water or water containing 0.5 wt % CTAB using a homogenizer. After slow evaporation of chloroform, various morphologies of BCP particles were obtained depending on the types of GQD surfactants used.

PS-*b*-P4VP(PDP)$_{0.5}$ particles in parts (a) and (b) of Figure 1 were prepared with GQD-HEX$_{0.7}$ and GQD-OLA$_{0.7}$, respectively. The feed volume fraction of GQDs (ϕ_{GQD}) in (GQD + PS-*b*-P4VP(PDP)$_{0.5}$) was 0.06, and GQD was used as sole surfactant without the addition of any other surfactant molecules (e.g., CTAB) in this case. Both GQD surfactants stabilized the BCP emulsions effectively due to their amphiphilic properties, and they generated the same spherical BCP particles with coiled, cylindrical morphology, as shown in Figure 1. However, the BCP particles had different outermost layers of PS and P4VP(PDP) polymers, depending on the types of GQD surfactants. The use of GQD-HEX$_{0.7}$ produced spherical BCP particles with preferential wetting of the PS layer to the particle surface. In contrast, GQD-OLA$_{0.7}$ generated BCP particles in which the P4VP(PDP) layer was exposed to the surface of the BCP particles (Figure 1b). This feature indicates that GQD-HEX$_{0.7}$ has preferred interaction with the PS domain, whereas there is strong favorable

DOI: 10.1021/acs.chemmater.5b04222
Chem. Mater. XXXX, XXX, XXX−XXX

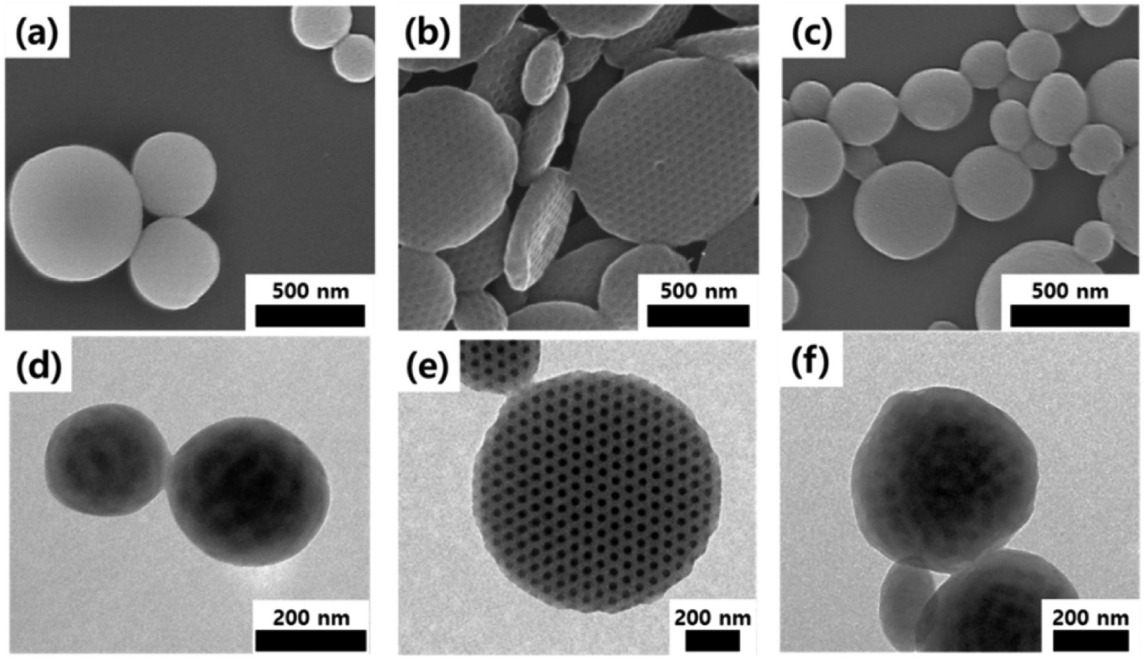

Figure 2. SEM and TEM images of PS-*b*-P4VP(PDP)$_{0.5}$ BCP particles without GQDs (a, d), with the addition of GQD-OLA$_{0.7}$ (b, e) and GQD-HEX$_{0.7}$ (c, f) at ϕ_{GQD} = 0.03. All of the emulsions were prepared in DI water containing 0.5 wt % CTAB.

interaction between GQD-OLA$_{0.7}$ and P4VP(PDP) domain. It has previously been demonstrated that OLA-coated NPs have strong favorable interactions with the aliphatic chain of PDP.[25,26] XPS measurements were also conducted to provide clear characterization of the outermost layers of the BCP particles. In the C 1s XPS spectra, both BCP particles show a strong peak at 285 eV because of the phenyl groups in the polymer backbone (Figure S4a). In contrast, when compared with N 1s XPS spectra at 399 eV, the strong intensity was observed only for GQD-OLA$_{0.7}$-stabilized BCP particles, confirming the presence of pyridine groups from the P4VP-(PDP) domains at the surface of BCP particles (Figure S4b).

Controlling the interaction between BCPs and the surrounding medium can be achieved by using a mixture of two different surfactants that have different affinities for each block of the BCP chain. First, when the BCP solution was emulsified by the most common cationic surfactant, CTAB as the sole surfactant, spherical BCP particles with cylindrical internal morphology were formed with a PS outermost layer due to the favorable interaction between the aliphatic tail of CTAB and PS chains (Figure 2a,d), which is in excellent agreement with previous observations.[25,26] In contrast, when a mixture of GQD-OLA$_{0.7}$ and CTAB was used, a dramatic transition in the overall shape of the BCP particles from spherical to a convex lens shape was observed. As shown in Figure 2b, a mixture of GQD-OLA$_{0.7}$ and CTAB surfactants resulted in CL particles with hexagonally packed dimples on the surface. During the purification step of the BCP particles with water, small PDP molecules within the P4VP(PDP) domain were extracted through the water phase, leading to the formation of dimple structures on the surface of the BCP particles. Figure 2e shows the TEM images of the particles with hexagonally packed, dark P4VP(PDP) domains, which demonstrates that the vertical cylinders were developed inside the particles. The mean diameter of the P4VP(PDP)$_{0.5}$ cylinders and the center-to-center distance between the cylinders were measured as 27.3 ± 2.5 and 57.8 ± 1.9 nm, respectively. These axially stacked P4VP(PDP) cylinders were clearly characterized in the tilted TEM images shown in Figure S5. Although the exact location of the GQDs cannot be visualized due to their very weak contrast with polymer particles, it is expected that most of the GQDs were located at the surface of the BCP particles, particularly segregated on the P4VP(PDP) domain. The relative size ratio (d/L) of GQD surfactants (d = 12.0 nm) to the P4VP(PDP)$_{0.5}$ domain size (L = 27.3 nm) was large enough (d/L > 0.4) to induce very large entropic penalty associated with the stretching of BCP chains to host large-sized GQDs.[26,44−48] In addition, the entropic penalty of the BCP chains can be amplified when the GQDs, with their platelike geometry, were confined in the cylindrical domains. Therefore, GQD surfactants were excluded from the P4VP(PDP) cylindrical domains and moved to the BCP emulsion/water interface, but they were located on the P4VP(PDP) domain at the particle surface. In contrast, other CTAB surfactants interacted preferentially with the PS domains of the PS-*b*-P4VP(PDP) at the particle surface. This preference could generate a balanced interaction between the PS/P4VP domains of the BCP particles and the surrounding water during emulsification.[26,28] When both the PS and P4VP(PDP) domains are exposed to the surfaces of the BCP particles, PS-*b*-P4VP(PDP) will self-assemble in a way with low curvature boundaries to minimize the entropic penalty associated with bending the BCP chains. In this case, the difference in the packing structure of the BCP chains at the lateral surface and end surface of the BCP droplets induces the mismatch in the surface energies at different positions (Figure S6). This difference in the surface energy provides the transition in the overall shape of the BCP particles from the spherical shape to the CL shape.[49]

In stark contrast, a mixture of both CTAB and GQD-HEX$_{0.7}$ produced only spherical BCP particles with the PS outermost layer as a consequence of preferential wetting of the PS layer to the surface of the particles (Figure 2c,f). To demonstrate the importance of the selective interaction of GQD-OLA$_{0.7}$ with the

DOI: 10.1021/acs.chemmater.5b04222
Chem. Mater. XXXX, XXX, XXX−XXX

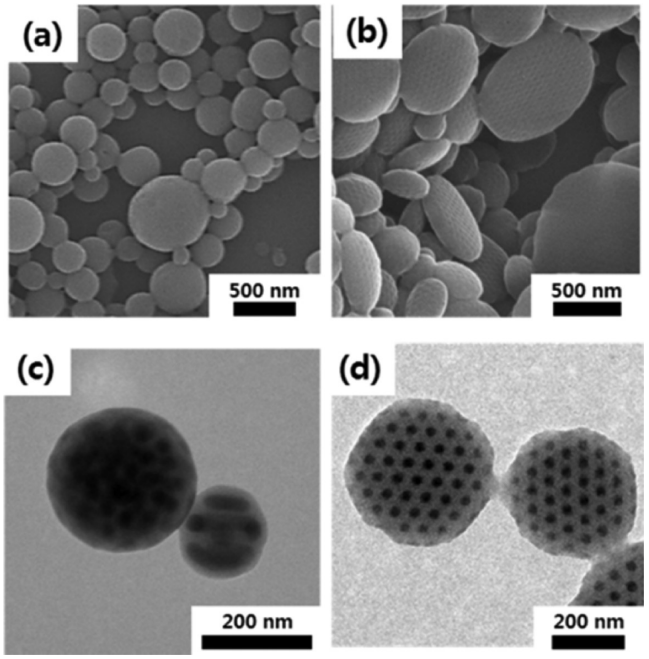

Figure 3. SEM and TEM images of PS-*b*-P4VP(PDP)$_{0.5}$ particles, obtained with GQD-OLA$_{0.2}$ ((a) and (c)) and GQD-OLA$_{0.7}$ ((b) and (d)). The ϕ_{GQD} value was fixed at 0.02. The particles were produced by emulsifying the polymer solution in DI water containing 0.5 wt % CTAB.

P4VP(PDP) domains in producing CL particles, we performed a control experiment. PS-*b*-P4VP colloidal particles were prepared using GQD-OLA$_{0.7}$ under identical conditions, but the PDP molecules were not added to the polymer solution. Unlike the PS-*b*-P4VP(PDP)$_{0.5}$ BCP particles, the PS-*b*-P4VP BCP particles showed spherical BCP particles without any morphological transition (Figure S7). In this case, the interaction between GQD-OLA$_{0.7}$ and P4VP domain was very weak, and it was insufficient to induce the selective positioning of GQDs in the P4VP domain.

Interestingly, even with a fixed type of ligand, fine-tuning of the surface properties of GQDs can be achieved by controlling the amount of the grafted organic ligands on the GQD surface. To demonstrate the importance of such delicate tuning of the surface properties of the GQDs, a series of GQD-OLAs with different OLA grafting densities (Σ) were obtained, which was achieved simply by controlling the feed ratios of OLA ligands to the GQDs during the surface modification step. As a result, three different GQDs were synthesized with the Σ values of 0.2 (GQD-OLA$_{0.2}$), 0.4 (GQD-OLA$_{0.4}$), and 0.7 (GQD-OLA$_{0.7}$) chain/nm^2, respectively. Then, the polymer solution and GQD-OLA with different Σ were emulsified in aqueous solutions including 0.5 wt % CTAB. Figure 3 compares the morphology of the BCP particles developed with two different GQD-OLA (GQD-OLA$_{0.2}$ and GQD-OLA$_{0.7}$) at a fixed GQD volume fraction (ϕ_{GQD}) of 0.02. As shown in Figure 3a,c, when GQD-OLA$_{0.2}$ was used, spherical BCP particles were obtained. In contrast, the addition of GQD-OLA$_{0.7}$ generated the morphological transition to CL particles (Figure 3b,d). This difference

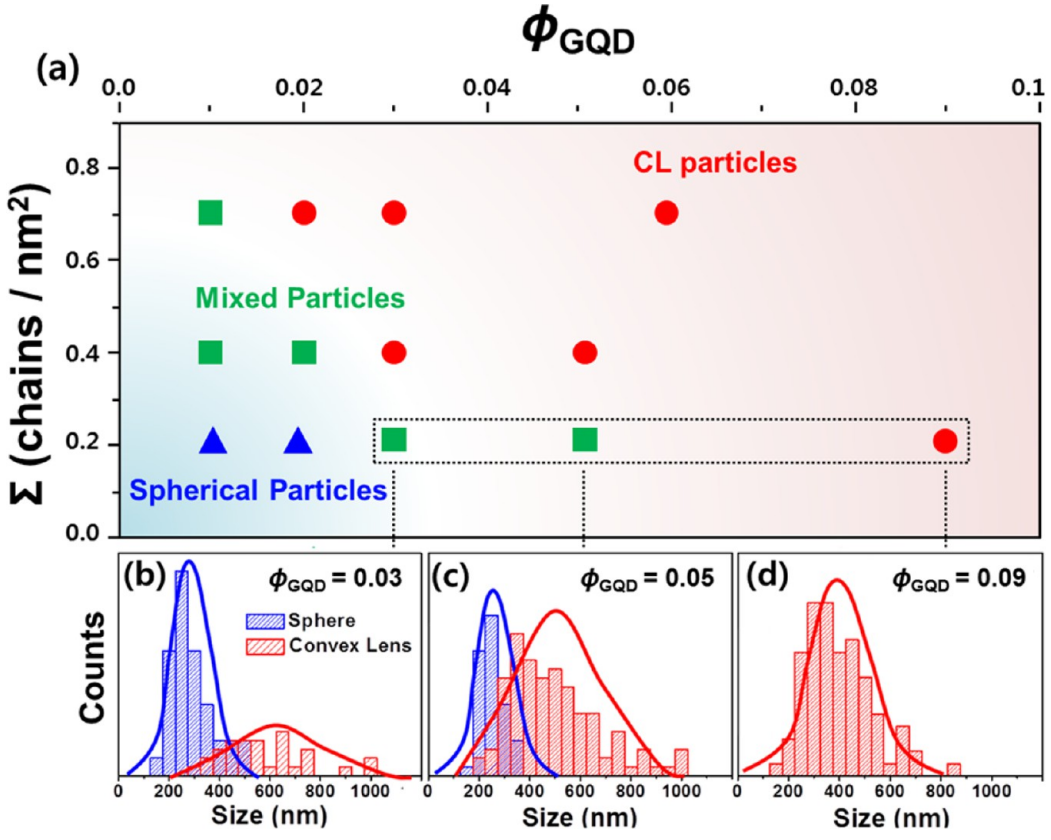

Figure 4. (a) Summary of the morphological behavior of PS-*b*-P4VP(PDP)$_{0.5}$ particles as functions of the Σ and ϕ_{GQD} values: (●, red) CL particles; (■, green) mixed particles; (▲, blue) spherical particles. All of the emulsions were emulsified in DI water containing 0.5 wt % CTAB. Histograms of size and shape distribution of the BCP particles produced by GQD-OLA$_{0.2}$ with ϕ_{GQD} values of (b) 0.03, (c) 0.05, and (d) 0.09.

DOI: 10.1021/acs.chemmater.5b04222
Chem. Mater. XXXX, XXX, XXX−XXX

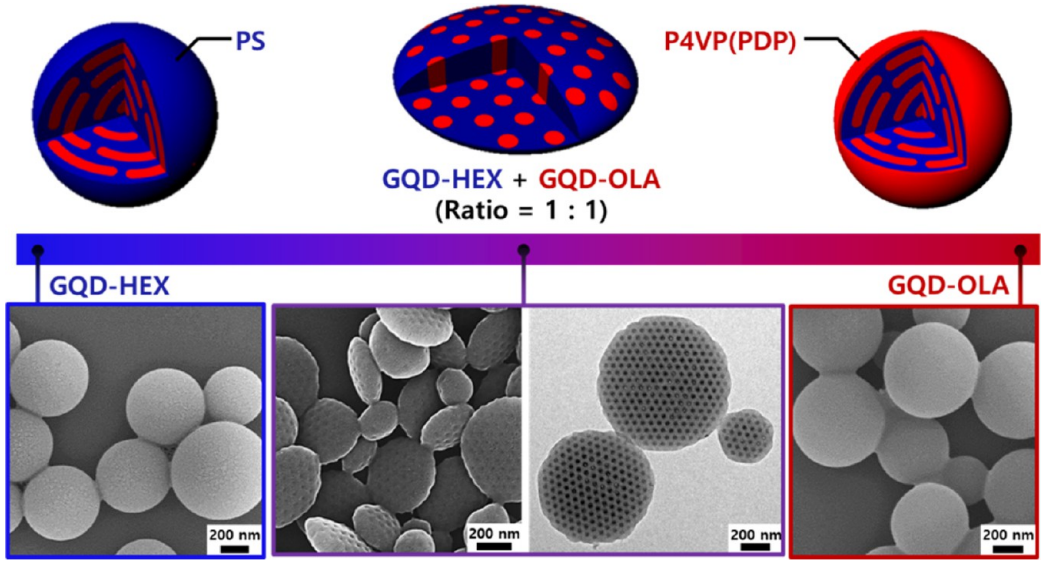

Figure 5. Phase behavior for the shape and internal structure of PS-*b*-P4VP(PDP)$_{0.5}$ particles stabilized by a mixture of GQD-OLA$_{0.7}$ and GQD-HEX$_{0.7}$. In this case, no CTAB molecules were added. The PS and P4VP(PDP) phases are represented as blue and red colors, respectively.

occurred because the interaction between the P4VP(PDP) domains and GQD-OLA$_{0.2}$ is much weaker than that between the P4VP(PDP) and GQD-OLA$_{0.7}$ due to the much lower density of OLA chains on the GQDs.

To fully understand the effect of GQD surfactants on the morphology of BCP particles, we examined the morphological behavior of the BCP particles containing GQD-OLA in terms of the Σ and ϕ_{GQD} values (Figure 4). For a given type of GQD, the parameter, ϕ_{GQD}, has significant influence in determining the particle shape. At high Σ (GQD-OLA$_{0.7}$), even small amounts of GQD surfactants (ϕ_{GQD} = 0.02) were sufficient to produce CL particles. In contrast, at low Σ (GQD-OLA$_{0.2}$), a large amount of GQD surfactants (ϕ_{GQD} > 0.09) were required to induce the morphological transition to CL particles. Particularly, for the case of GQD-OLA$_{0.2}$, we observed an interesting morphological behavior of the BCP particles at the intermediate regime of ϕ_{GQD} (0.02 < ϕ_{GQD} < 0.09). In this regime, the BCP particles included a mixture of spherical and CL particles (Figure S8). Interestingly, the shape of the BCP particles was strongly dependent on the particle size. In our experiment, BCP particles were produced using the homogenizer and, thus they had a wide variation in size, ranging from 200 to 1600 nm. With use of GQD-OLA$_{0.2}$ surfactants at ϕ_{GQD} = 0.03, the BCP particles smaller than 400 nm had spherical shapes, whereas the particles larger than 400 nm had convex lens shapes (Figure 4b). With the increase in the ϕ_{GQD} value from 0.03 to 0.05, a larger fraction of the BCP particles had convex-lens shape, showing that most of the BCP particles larger than 300 nm had changed to CL particles. Also, the average size of the spherical particles decreased from 320 to 270 nm (Figure 4c). When the ϕ_{GQD} value increased to 0.09, all of the BCP particles converted to convex-lens shape (Figure 4d). The size-dependent shape of the BCP particles can be understood by comparing the surface coverage of GQDs (C_{GQD}) on the particle surface at different particle sizes. At a given ϕ_{GQD} value of the same emulsion batch, the C_{GQD} value on the BCP particle should scale relative to the diameter (d) of BCP emulsion droplets ($C_{GQD} \sim d$), assuming the same fraction of added GQDs is segregated at the particle surface. Thus, a higher ϕ_{GQD} value is required for smaller BCP particle to achieve a comparable C_{GQD} value that is required for the transition of the BCP particles.[28] Furthermore, the shape anisotropy of the BCP particles was strongly dependent on the particle size. This occurred because the particle size influenced the contributions from the interfacial energies of (i) the PS/P4VP(PDP), and (ii) PS-P4VP(PDP)/surrounding media, and (iii) the stretching and bending penalties of the BCP chains within the particles, which were important factors to determine the particle shape.[16,28] To investigate the effect of the particle size on the shape anisotropy of the CL particles, the aspect ratio L/S (L and S are the lengths of the long and short axes of the CL particles, respectively) as a function of the size (L) of the CL particles was examined as shown in Figure S9. It is evident that the elongation of particles increased as the L increased because the contributions from the interfacial energies (the terms (i) and (ii)) became more dominant. This observation is consistent with the results of Hawker and Kramer groups.[16,28]

To exploit the full potential of the surface-tailored GQD as surfactants, we developed BCP particles with a mixture of different GQD surfactants. As discussed in Figure 1, GQD-HEX and GQD-OLA have different preferential interaction with each block of PS-*b*-P4VP(PDP)$_{0.5}$. This ability to switch the outer layer by a choice of surfactants suggests that a neutral layer can also be obtained by adjusting the composition of the GQD mixture. To test this hypothesis, the polymer solution with the mixture of GQD-HEX$_{0.7}$ (ϕ_{GQD} = 0.06) and GQD-OLA$_{0.7}$ (ϕ_{GQD} = 0.06) was emulsified in water. As shown in Figure 5, a mixture of GQD-OLA$_{0.7}$ and GQD-HEX$_{0.7}$ successfully induced a morphological transition to CL particles. This result clearly demonstrates that the interfacial interactions between the BCP particle surface and the surrounding medium could be systematically modulated using surface-engineered GQD surfactants without any other surfactants. Therefore, the key to the successful control of the shape of the BCP particles was surface engineering of 10 nm-sized GQDs by alkyl ligands with controlled Σ, which was critical for precise positioning of GQDs at the particle surface and determining the surfactant efficiency in emulsions.

DOI: 10.1021/acs.chemmater.5b04222
Chem. Mater. XXXX, XXX, XXX−XXX

CONCLUSIONS

We described the feasibility of using GQDs as efficient surfactants in tailoring the shape and nanomorphology of BCP particles. Precise control of the surface properties of the GQDs was achieved by grafting alkyl ligands at a controlled density. In particular, the specific choice of OLA ligands on the GQDs is critically important in modulating the interfacial interactions between BCP particles and the surrounding media, leading to a neutral wetting of PS and P4VP(PDP) at the particle surface required for tuning the particle shape. Thus, addition of GQD-OLA to the BCP particles containing cylinder-forming PS-*b*-P4VP(PDP) polymers resulted in a dramatic transition from conventional spherical shape to CL particles. A complete picture for the morphology of the BCP particles was drawn in terms of the types of alkyl ligands on GQDs, and the Σ and ϕ_{GQD} values, which demonstrates the potential of GQD surfactants in producing shape-controlled colloidal particles with interesting luminescent and electrical properties.

ASSOCIATED CONTENT

Supporting Information

The Supporting Information is available free of charge on the ACS Publications website at DOI: 10.1021/acs.chemmater.5b04222.

Additional TEM images of GQD-stabilized BCP particles, and TEM, TGA, and ATR-FTIR results of alkylamine-grafted GQDs are included (PDF)

AUTHOR INFORMATION

Corresponding Author

*E-mail: bumjoonkim@kaist.ac.kr.

Notes

The authors declare no competing financial interest.

ACKNOWLEDGMENTS

This research was supported by the National Research Foundation Grant (2013R1A2A1A03069803), funded by the Korean Government.

REFERENCES

(1) Jin, Z. X.; Fan, H. L. Self-assembly of nanostructured block copolymer nanoparticles. *Soft Matter* **2014**, *10*, 9212−9219.

(2) Bockstaller, M.; Kolb, R.; Thomas, E. L. Metallodielectric photonic crystals based on diblock copolymers. *Adv. Mater.* **2001**, *13*, 1783−1786.

(3) Setaro, A.; Lettieri, S.; Maddalena, P.; De Stefano, L. Highly sensitive optochemical gas detection by luminescent marine diatoms. *Appl. Phys. Lett.* **2007**, *91*, 051921.

(4) Lu, Z. H.; Liu, G. J.; Phillips, H.; Hill, J. M.; Chang, J.; Kydd, R. A. Palladium nanoparticle catalyst prepared in poly(acrylic acid)-lined channels of diblock copolymer microspheres. *Nano Lett.* **2001**, *1*, 683−687.

(5) Ku, K. H.; Kim, M. P.; Paek, K.; Shin, J. M.; Chung, S.; Jang, S. G.; Chae, W. S.; Yi, G. R.; Kim, B. J. Multicolor Emission of Hybrid Block Copolymer-Quantum Dot Microspheres by Controlled Spatial Isolation of Quantum Dots. *Small* **2013**, *9*, 2667−2672.

(6) Groschel, A. H.; Schacher, F. H.; Schmalz, H.; Borisov, O. V.; Zhulina, E. B.; Walther, A.; Muller, A. H. E. Precise hierarchical self-assembly of multicompartment micelles. *Nat. Commun.* **2012**, *3*, 710.

(7) Zhu, J.; Ferrer, N.; Hayward, R. C. Tuning the assembly of amphiphilic block copolymers through instabilities of solvent/water interfaces in the presence of aqueous surfactants. *Soft Matter* **2009**, *5*, 2471−2478.

(8) Zhu, J.; Hayward, R. C. Hierarchically structured microparticles formed by interfacial instabilities of emulsion droplets containing amphiphilic block copolymers. *Angew. Chem., Int. Ed.* **2008**, *47*, 2113−2116.

(9) Konishi, N.; Fujibayashi, T.; Tanaka, T.; Minami, H.; Okubo, M. Effects of properties of the surface layer of seed particles on the formation of golf ball-like polymer particles by seeded dispersion polymerization. *Polym. J.* **2010**, *42*, 66−71.

(10) Okubo, M.; Saito, N.; Takekoh, R.; Kobayashi, H. Morphology of poly styrene/polystyrene-block-poly(methyl methacrylate)/poly-(methyl methacrylate) composite particles. *Polymer* **2005**, *46*, 1151−1156.

(11) Jeon, S. J.; Yi, G. R.; Koo, C. M.; Yang, S. M. Nanostructures inside colloidal particles of block copolymer/homopolymer blends. *Macromolecules* **2007**, *40*, 8430−8439.

(12) Li, L.; Matsunaga, K.; Zhu, J.; Higuchi, T.; Yabu, H.; Shimomura, M.; Jinnai, H.; Hayward, R. C.; Russell, T. P. Solvent-Driven Evolution of Block Copolymer Morphology under 3D Confinement. *Macromolecules* **2010**, *43*, 7807−7812.

(13) Shin, J. M.; Kim, M. P.; Yang, H.; Ku, K. H.; Jang, S. G.; Youm, K. H.; Yi, G.-R.; Kim, B. J. Monodipserse Nanostructured Spheres of Block Copolymers and Nanoparticles via Cross-Flow Membrane Emulsification. *Chem. Mater.* **2015**, *27*, 6314−6321.

(14) Yu, B.; Li, B. H.; Jin, Q. H.; Ding, D.; Shi, A. C. Self-assembly of symmetric diblock copolymers confined in spherical nanopores. *Macromolecules* **2007**, *40*, 9133−9142.

(15) Jeon, S. J.; Yi, G. R.; Yang, S. M. Cooperative Assembly of Block Copolymers with Deformable Interfaces: Toward Nanostructured Particles. *Adv. Mater.* **2008**, *20*, 4103−4108.

(16) Klinger, D.; Wang, C. X.; Connal, L. A.; Audus, D. J.; Jang, S. G.; Kraemer, S.; Killops, K. L.; Fredrickson, G. H.; Kramer, E. J.; Hawker, C. J. A Facile Synthesis of Dynamic, Shape-Changing Polymer Particles. *Angew. Chem., Int. Ed.* **2014**, *53*, 7018−7022.

(17) Xu, J. P.; Wang, K.; Li, J. Y.; Zhou, H. M.; Xie, X. L.; Zhu, J. ABC Triblock Copolymer Particles with Tunable Shape and Internal Structure through 3D Confined Assembly. *Macromolecules* **2015**, *48*, 2628−2636.

(18) Rahikkala, A.; Soininen, A. J.; Ruokolainen, J.; Mezzenga, R.; Raula, J.; Kauppinen, E. I. Self-assembly of PS-b-P4VP block copolymers of varying architectures in aerosol nanospheres. *Soft Matter* **2013**, *9*, 1492−1499.

(19) Yan, N.; Liu, H.; Zhu, Y.; Jiang, W.; Dong, Z. Entropy-Driven Hierarchical Nanostructures from Cooperative Self-Assembly of Gold Nanoparticles/Block Copolymers under Three-Dimensional Confinement. *Macromolecules* **2015**, *48*, 5980−5987.

(20) Kim, M. P.; Kang, D. J.; Jung, D. W.; Kannan, A. G.; Kim, K. H.; Ku, K. H.; Jang, S. G.; Chae, W. S.; Yi, G. R.; Kim, B. J. Gold-Decorated Block Copolymer Microspheres with Controlled Surface Nanostructures. *ACS Nano* **2012**, *6*, 2750−2757.

(21) Deng, R. H.; Liu, S. Q.; Li, J. Y.; Liao, Y. G.; Tao, J.; Zhu, J. Mesoporous Block Copolymer Nanoparticles with Tailored Structures by Hydrogen-Bonding-Assisted Self-Assembly. *Adv. Mater.* **2012**, *24*, 1889−1893.

(22) Kim, M. P.; Ku, K. H.; Kim, H. J.; Jang, S. G.; Yi, G. R.; Kim, B. J. Surface Intaglio Nanostructures on Microspheres of Gold-Cored Block Copolymer Spheres. *Chem. Mater.* **2013**, *25*, 4416−4422.

(23) Tanaka, T.; Saito, N.; Okubo, M. Control of Layer Thickness of Onionlike Multilayered Composite Polymer Particles Prepared by the Solvent Evaporation Method. *Macromolecules* **2009**, *42*, 7423−7429.

(24) Deng, R. H.; Liang, F. X.; Li, W. K.; Yang, Z. Z.; Zhu, J. Reversible Transformation of Nanostructured Polymer Particles. *Macromolecules* **2013**, *46*, 7012−7017.

(25) Ku, K. H.; Yang, H.; Shin, J. M.; Kim, B. J. Aspect Ratio Effect of Nanorod Surfactants on the Shape and Internal Morphology of Block Copolymer Particles. *J. Polym. Sci., Part A: Polym. Chem.* **2015**, *53*, 188−192.

DOI: 10.1021/acs.chemmater.5b04222
Chem. Mater. XXXX, XXX, XXX−XXX

(26) Ku, K. H.; Shin, J. M.; Kim, M. P.; Lee, C. H.; Seo, M. K.; Yi, G. R.; Jang, S. G.; Kim, B. J. Size-Controlled Nanoparticle-Guided Assembly of Block Copolymers for Convex Lens-Shaped Particles. *J. Am. Chem. Soc.* **2014**, *136*, 9982−9989.
(27) Schmidt, B. V. K. J.; Elbert, J.; Scheid, D.; Hawker, C. J.; Klinger, D.; Gallei, M. Metallopolymer-Based Shape Anisotropic Nanoparticles. *ACS Macro Lett.* **2015**, *4*, 731−735.
(28) Jang, S. G.; Audus, D. J.; Klinger, D.; Krogstad, D. V.; Kim, B. J.; Cameron, A.; Kim, S. W.; Delaney, K. T.; Hur, S. M.; Killops, K. L.; Fredrickson, G. H.; Kramer, E. J.; Hawker, C. J. Striped, Ellipsoidal Particles by Controlled Assembly of Diblock Copolymers. *J. Am. Chem. Soc.* **2013**, *135*, 6649−6657.
(29) Zhang, Z. P.; Zhang, J.; Chen, N.; Qu, L. T. Graphene quantum dots: an emerging material for energy-related applications and beyond. *Energy Environ. Sci.* **2012**, *5*, 8869−8890.
(30) Shen, J. H.; Zhu, Y. H.; Yang, X. L.; Li, C. Z. Graphene quantum dots: emergent nanolights for bioimaging, sensors, catalysis and photovoltaic devices. *Chem. Commun.* **2012**, *48*, 3686−3699.
(31) Cho, H.-H.; Yang, H.; Kang, D. J.; Kim, B. J. Surface Engineering of Graphene Quantum Dots and Their Applications as Efficient Surfactants. *ACS Appl. Mater. Interfaces* **2015**, *7*, 8615−8621.
(32) Yang, H.; Kang, D. J.; Ku, K. H.; Cho, H. H.; Park, C. H.; Lee, J.; Lee, D. C.; Ajayan, P. M.; Kim, B. J. Highly Luminescent Polymer Particles Driven by Thermally Reduced Graphene Quantum Dot Surfactants. *ACS Macro Lett.* **2014**, *3*, 985−990.
(33) Vis, M.; Opdam, J.; van 't Oor, I. S. J.; Soligno, G.; van Roij, R.; Tromp, R. H.; Erné, B. H. Water-in-Water Emulsions Stabilized by Nanoplates. *ACS Macro Lett.* **2015**, *4*, 965−968.
(34) Creighton, M. A.; Ohata, Y.; Miyawaki, J.; Bose, A.; Hurt, R. H. Two-Dimensional Materials as Emulsion Stabilizers: Interfacial Thermodynamics and Molecular Barrier Properties. *Langmuir* **2014**, *30*, 3687−3696.
(35) Park, C. H.; Yang, H.; Lee, J.; Cho, H. H.; Kim, D.; Lee, D. C.; Kim, B. J. Multicolor Emitting Block Copolymer-Integrated Graphene Quantum Dots for Colorimetric, Simultaneous Sensing of Temperature, pH, and Metal Ions. *Chem. Mater.* **2015**, *27*, 5288−5294.
(36) Zhu, S. J.; Zhang, J. H.; Tang, S. J.; Qiao, C. Y.; Wang, L.; Wang, H. Y.; Liu, X.; Li, B.; Li, Y. F.; Yu, W. L.; Wang, X. F.; Sun, H. C.; Yang, B. Surface Chemistry Routes to Modulate the Photoluminescence of Graphene Quantum Dots: From Fluorescence Mechanism to Up-Conversion Bioimaging Applications. *Adv. Funct. Mater.* **2012**, *22*, 4732−4740.
(37) Kim, B. J.; Bang, J.; Hawker, C. J.; Kramer, E. J. Effect of areal chain density on the location of polymer-modified gold nanoparticles in a block copolymer template. *Macromolecules* **2006**, *39*, 4108−4114.
(38) Kim, B. J.; Fredrickson, G. H.; Hawker, C. J.; Kramer, E. J. Nanoparticle surfactants as a route to bicontinuous block copolymer morphologies. *Langmuir* **2007**, *23*, 7804−7809.
(39) Ye, Y. S.; Chen, Y. N.; Wang, J. S.; Rick, J.; Huang, Y. J.; Chang, F. C.; Hwang, B. J. Versatile Grafting Approaches to Functionalizing Individually Dispersed Graphene Nanosheets Using RAFT Polymerization and Click Chemistry. *Chem. Mater.* **2012**, *24*, 2987−2997.
(40) Yang, H.; Paek, K.; Kim, B. J. Efficient Temperature Sensing Platform Based on Fluorescent Block Copolymer-Functionalized Graphene Oxide. *Nanoscale* **2013**, *5*, 5720−5724.
(41) Dong, Y. Q.; Chen, C. Q.; Zheng, X. T.; Gao, L. L.; Cui, Z. M.; Yang, H. B.; Guo, C. X.; Chi, Y. W.; Li, C. M. One-step and high yield simultaneous preparation of single- and multi-layer graphene quantum dots from CX-72 carbon black. *J. Mater. Chem.* **2012**, *22*, 8764−8766.
(42) Wang, D.; Zhu, L.; Chen, J. F.; Dai, L. M. Can graphene quantum dots cause DNA damage in cells? *Nanoscale* **2015**, *7*, 9894−9901.
(43) Zhao, Y.; Thorkelsson, K.; Mastroianni, A. J.; Schilling, T.; Luther, J. M.; Rancatore, B. J.; Matsunaga, K.; Jinnai, H.; Wu, Y.; Poulsen, D.; Frechet, J. M. J.; Alivisatos, A. P.; Xu, T. Small-molecule-directed nanoparticle assembly towards stimuli-responsive nanocomposites. *Nat. Mater.* **2009**, *8*, 979−985.
(44) Thompson, R. B.; Ginzburg, V. V.; Matsen, M. W.; Balazs, A. C. Predicting the mesophases of copolymer-nanoparticle composites. *Science* **2001**, *292*, 2469−2472.
(45) Bockstaller, M. R.; Lapetnikov, Y.; Margel, S.; Thomas, E. L. Size-selective organization of enthalpic compatibilized nanocrystals in ternary block copolymer/particle mixtures. *J. Am. Chem. Soc.* **2003**, *125*, 5276−5277.
(46) Spontak, R. J.; Shankar, R.; Bowman, M. K.; Krishnan, A. S.; Hamersky, M. W.; Samseth, J.; Bockstaller, M. R.; Rasmussen, K. O. Selectivity- and size-induced segregation of molecular and nanoscale species in microphase-ordered triblock copolymers. *Nano Lett.* **2006**, *6*, 2115−2120.
(47) Kao, J.; Bai, P.; Lucas, J. M.; Alivisatos, A. P.; Xu, T. Size-Dependent Assemblies of Nanoparticle Mixtures in Thin Films. *J. Am. Chem. Soc.* **2013**, *135*, 1680−1683.
(48) Kao, J.; Bai, P.; Chuang, V. P.; Jiang, Z.; Ercius, P.; Xu, T. Nanoparticle Assemblies in Thin Films of Supramolecular Nanocomposites. *Nano Lett.* **2012**, *12*, 2610−2618.
(49) Koizumi, S.; Hasegawa, H.; Hashimoto, T. Ordered Structures of Block Copolymer/Homopolymer Mixtures 0.5. Interplay of Macrophase and Microphase Transitions. *Macromolecules* **1994**, *27*, 6532−6540.

DOI: 10.1021/acs.chemmater.5b04222
Chem. Mater. XXXX, XXX, XXX−XXX